THE ASTROPHYSICAL JOURNAL, 194:569–585, 1974 December 15

AN INTERPRETATION OF RING GALAXIES AND THE PROPERTIES OF INTERGALACTIC GAS CLOUDS

K. C. FREEMAN
Mount Stromlo and Siding Spring Observatory, Australian National University, Canberra
AND
G. DE VAUCOULEURS
McDonald Observatory, The University of Texas at Austin
Received 1974 April 8

ABSTRACT

We propose that the pairs of peculiar spheroidal galaxies associated with ring-type objects (e.g., IC 298 = Arp 147) or chaotic multinucleated objects (e.g., NGC 2444–5 = Arp 143) result from encounters of normal spirals with intergalactic H I clouds. Observational constraints restrict the cloud parameters to a small range around $\mathfrak{M} = 3 \times 10^9\ \mathfrak{M}_\odot$, $R = 15$ kpc, $N = 25\ \mathrm{Mpc}^{-3}$. A significant fraction of normal lenticular galaxies and of late-type Magellanic irregulars could have been produced by such galaxy-cloud encounters, as remnants of respectively the old stellar component and of the gas disk component. We suggest that some "isolated extragalactic H II regions" (e.g., I Zw 18 and II Zw 40) could result from cloud-cloud encounters. Specific models of individual peculiar galaxies based on this concept are presented.

Subject headings: galaxies — intergalactic medium

I. INTRODUCTION

In this paper we propose a simple interpretation and formation mechanism for two related types of pairs of peculiar galaxies consisting of a spheroidal system and either (*a*) the rare and curious pure ring-type galaxies, like IC 298 = Arp 147 (Arp 1966), or (*b*) the chaotic multinucleated objects, like NGC 2444–5 = VV 117 = Arp 143. Table 1 lists some of the best known examples. These two classes of peculiar galaxies share several characteristics:

1. An early-type system, resembling an elliptical or lenticular galaxy (component A) is associated with a late-type ring-shaped or chaotic object (component B).
2. The angular separation S of the two components is of the same order as the diameter D of the ring-shaped or chaotic component. The appearance often suggests tidal interaction, and the radial velocity differential between the two components is usually small (100–200 km s^{-1}); their linear separation is then also small. From table 1 and with distances estimated from redshifts $\langle S/D \rangle \simeq 0.9$ ($n = 12$), $\langle S \rangle \simeq 8.4h^{-1}$ kpc ($n = 8$), and $\langle D \rangle \simeq 11.5h^{-1}$ kpc ($n = 9$), where $h = H/100$.
3. The shape of the ring in type (*a*) objects varies from nearly circular (IC 298) to highly elliptical (NGC 4774). This means that the ring is most likely a flat circular annulus or torus.
4. The chaotic component in type (*b*) objects is frequently pear-shaped, almost triangular, and often with one or more condensations near its center.

Several tentative explanations for these systems have already been advanced. For example, Burbidge and Burbidge (1959) suggest as possibilities "the aftermath of a close collision between an elliptical and a spiral," or perhaps "the formation of a new galaxy in the wake of another older system," as in the steady-state picture. More recently, Freeman and Woolf[1] compared such objects with eddy patterns in laboratory studies of fluid flows at intermediate Reynolds number. Sérsic (1970) considered the formation of transient annular structures or "Lagrangian rings" in the ejecta of an exploding galaxy, while Cannon, Lloyd, and Penston (1970) proposed that they may "represent the disk material of galaxies . . . separated from their nuclei by interaction with another galaxy."

We present here another explanation which accounts for both (*a*) and (*b*) type systems by combining several aspects of previous suggestions with a more plausible formation mechanism and a more detailed consideration of the subsequent evolution. In § II we give a qualitative account of the process, and in § III we discuss the observational constraints and estimate orders of magnitude for the physical parameters.

II. FORMATION AND EVOLUTION OF THE RING

a) Formation

We postulate first the existence of moderately dense intergalactic gas clouds (IGC) which we will assume to be neutral hydrogen clouds; evidence for such clouds comes from the H I clouds of galactic dimensions in the M31 and M81 groups (Davies 1973), the H I companion to NGC 300 (Shobbrook and Robinson 1967), and the Magellanic Stream (Mathewson, Cleary, and Murray 1973). (While we are making the working hypothesis that the clouds are neutral gas, the main concept of this paper does not specifically require the

[1] Unpublished; but the concept was illustrated by a photomontage reproduced in Menzel, Whipple, and de Vaucouleurs (1973).

TABLE 1

RING GALAXIES

OBJECT	ARP ATLAS	TYPE	Corr. Vel. V_0 A	Corr. Vel. V_0 A + B	Corr. Vel. V_0 B	S″ = kpc*	D″ × d″ = kpc*	S/D	V_{AB} V_A V_B	$(B-V)_{AB}$ $(B-V)_A$ $(B-V)_B$	$(U-B)_{AB}$ $(U-B)_A$ $(U-B)_B$	Remarks
N1143–4.....	118	b?	...		...	32	30 × 15:	1.1	12.4[j]	+0.94[j]	+0.30[j]	
									...	...	...	
									...	...	...	
VV 123.....	141	b	2996[a]		...	55 =	60 × 30 =	0.9	...	...	...	
			2673[b]		...	8.0	8.7		...	+0.90[j]	+0.30[j]	
									...	...	...	(1)
N2936–7 = VV 316...	142	b	6709[b]		6849[b]	24 =	65 × 40: =	0.4	...	...	...	
			6680[c]		6980[c]	8.0	21.5		...	...	...	
			6736[d]		7202[d]				...	...	...	
N2444–5 = VV 117...	143	b	3949[e]		4101[e]	64 =	80: × 50: =	0.8	12.13[k]	+0.77[k]	+0.12[k]	
						12.5	15.7		13.59[k]	+1.01[k]	+0.53[k]	
									13.33[k]	+0.63[k]	−0.01[k]	(2)
N7828–9 = VV 272...	144	a?	5748[c]		5880[c]	40: =	33: = 9.3	...	...	...	...	
						11			...	...	...	
									...	...	...	
A0221+51 = V Zw 229.....	145	b	5388[f]		...	35 =	60 × 42 =	0.6	14.68[k]	+0.81[k]	+0.76[k]	
			5476[b]			9.1	15.5		14.98[k]	+0.96[k]	+0.21[k]	
									...	...	...	
A0005−06.....	146	a	...		...	13	18 × 10	0.7	14.66[k]	+1.0:[k]	...	
									15.66[k]	+0.6:[k]	...	
									15.85[k]	+0.6:[k]	...	
IC 298 = I Zw 11....	147	a	...	9424[f]	...	18 =	15 × 13 =	1.2	...	...	...	(3)
						8.2	6.8		...	...	...	
									...	...	...	
A1102+51 = Mayall's.....	148	ab	10356[g]		...	13 =	17 × 13 =	0.7_5	14.4:	+0.7:	−0.16	
			10374[h]		10612[h]	6.6	8.6		...	...	...	
									...	...	...	
A1238+16.....	149	b?	...		...	27	26 × 3:	1.0	...	...	...	
N6438.....	...	b	2573[i]		2402[i]	33: =	100: × 35: =	0.3:	...	...	...	
			2352[c]		2445[c]	3.9	11.8					
N4774 = I Zw 45....	...	a	...		...	25	30 × 15	0.8	...	...	...	(4)
A1229+66 = VII Zw 466.....	...	a	...		...	50	25 × 15	2.0	...	...	...	
A0459+03 = II Zw 28.....	...	a	...	8548[f]	...	...	13 × 10 = 5.4	...	...	...	...	
N985 = VV 285.....	...	a	...		...	...	...	...	...	...	...	

REMARKS.—(1) Component B nucleus $B-V=+0.45$, $U-B=+0.02$ (Sandage 1963). (2) Component B nucleus $B-V=+0.81$, $U-B\simeq+0.13$ (Sandage 1963). (3) Incorrectly listed as I Zw 10 by Sargent 1970. (4) Incorrectly listed as I Zw 44 by Cannon *et al.* 1970.

[a] E. M. Burbidge, quoted by Sandage 1963.
[b] Arp 1967.
[c] This paper (Mount Stromlo).
[d] Chincarini and Rood 1972.
[e] Burbidge and Burbidge 1959.
[f] Sargent 1970.
[g] Humason, Mayall, and Sandage 1956.
[h] Burbidge 1964.
[i] Burbidge 1972.
[j] Sandage 1963.
[k] This paper (McDonald).
* ($h=1$).

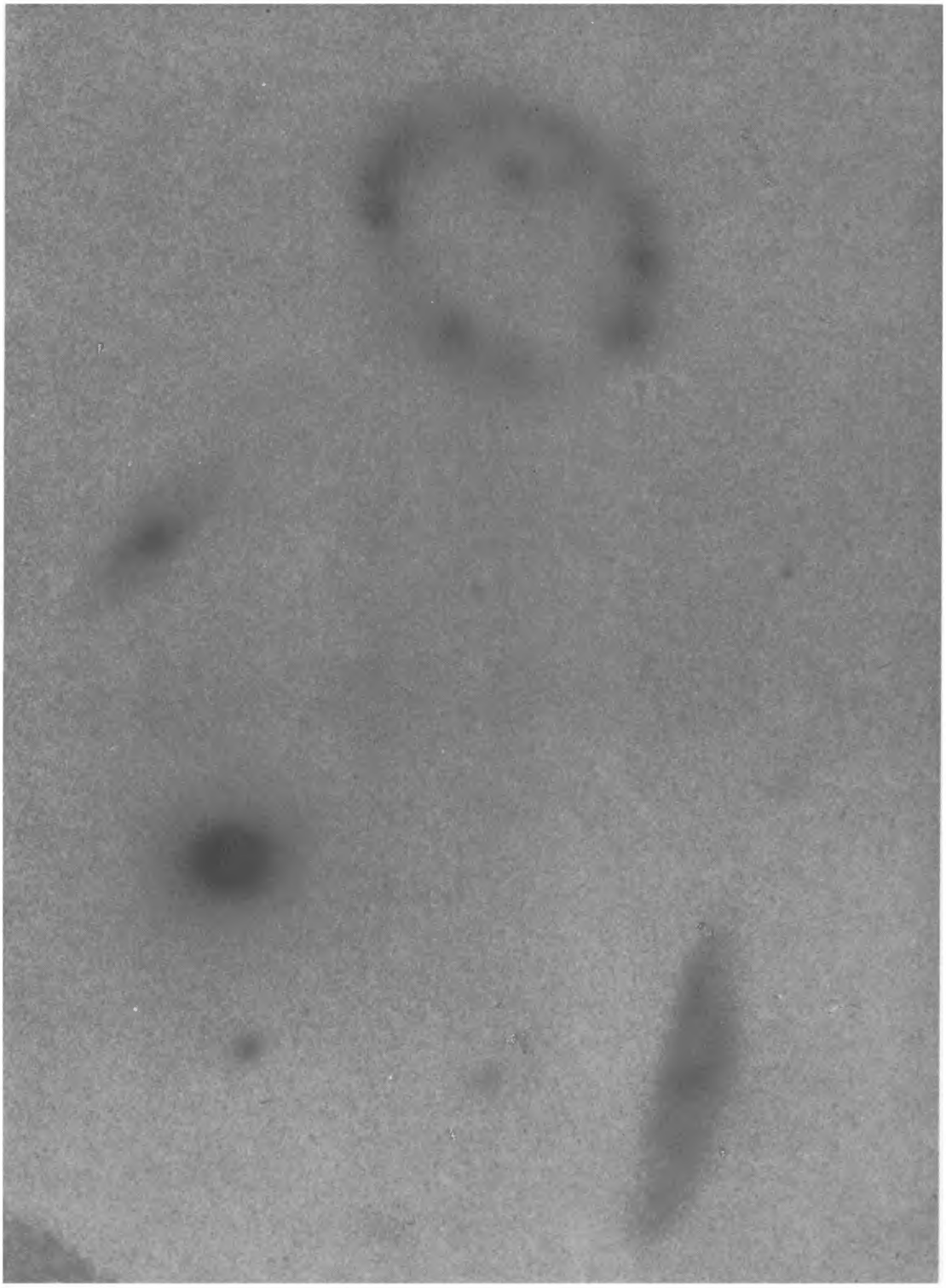

FIG. 1.—Ring galaxy VII Zw 466 photographed by G. Chincarini with Kron electronographic camera attached at Cassegrain focus of Struve 205-cm reflector, McDonald Observatory, April 29, 1973, Ilford K5, 95 mn, B filter. Elliptical-looking Component A is brightest object in field; two unrelated spirals in group are seen. Several large H II regions and probable associations are visible in ring Component B.

gas to be neutral or ionized; which of the two it is will need to be established by additional physical data.) We then note that the isophotes of typical *a*-type rings —for example, VII Zw 466 (figs. 1 and 2)—are remarkably similar to the equidensity contours of the annular zone of 21-cm emission in typical disk galaxies, e.g., M31 (Gottesman and Davies 1970; Baldwin 1974) or the Milky Way (Kerr and Westerhout 1965).

If such a disk galaxy were to suffer a near face-on collision with an IGC of sufficient density and depth, then two remarkable consequences should follow: (1) the central spheroidal component of the galaxy, and the *stellar* component of the disk, would pass almost undisturbed through the IGC; (2) the gaseous ring-shaped disk component would be slowed down and eventually brought to rest with respect to the IGC, within some distance that depends on relative masses, densities, and velocities; this distance is presumably less than the observed separation of several kiloparsecs between the two components of these systems. To fix ideas in a semiquantitative way, assume that the gas densities in the disk of the galaxy and in the IGC are comparable, and that the initial relative velocity V_0 of the galaxy to the cloud is 200 km s^{-1}. In about 10^7 yr, the gaseous disk will sweep up enough mass from the cloud to reduce the relative velocity to a small fraction of the initial velocity. Meanwhile, the stellar component will continue unimpeded and (after the initial 10^7 yr) will separate from the gas disk at a rate of about 2 kpc every 10^7 yr. For a typical giant spiral, for which the H I annulus may be some 10–20 kpc in diameter, the separation of components is equal to the ring diameter after about (5–10) $\times$ 10^7 yr. This time interval is also the order of magnitude of the original rotation period for the disk and of the free-fall time $(G\rho)^{-1/2}$ for the disk matter.

b) Evolution

A flat spinning gas ring is unstable, so we can expect two main phases in the evolution of the dismembered galaxy, as the time t after impact increases.

i) $t < 10^8$ yr. The separation of the two components is less than the diameter of the ring, which is still geometrically well preserved. The increasing gas density in the ring induces, after perhaps $\sim 10^7$ years, a burst of star formation leading to the observed high-luminosity H II regions and other extreme Population I characteristics of most *a*-type rings.

ii) $t > 10^8$ yr. The inherent instability of the ring leads to a collapse and chaotic reorganization of the material, presumably toward some kind of centrally condensed object. This process can account for the various examples of *b*-type systems. In particular, if the initial relative velocity V_0 is less than average, say $V_0 < 100$ km s^{-1}, the collapse phase of the gaseous component B will take place in strong interaction with the gravitational field of the more massive lenticular component A.

The model predicts two main sources of light emission from the rings. Initially, say for $t < 10^7$ yr, collisional excitation, ionization, and recombination of hydrogen should dominate. Later, for $t > 10^7$ yr, after star formation becomes significant, thermal emission from OB associations and radiative excitation of giant H II regions should be the main source of luminosity in the gaseous component, which for $t > 10^8$ yr may be evolving toward a more normal Magellanic irregular type of system. This concept appears to be consistent with available spectroscopic and colorimetric data (Sandage 1963; Freeman and Craft 1974).

The model also predicts that the ring should be richer in hydrogen than the gas in the disk of the initial galaxy, or relative to hydrogen an underabundance of heavy elements should characterize the spectrum of the ring compared with normal galaxy spectra. This appears to be consistent with spectroscopic observations of Mayall's nebula by Burbidge (1964), who remarked that "a strong Hα line appeared in the more luminous side of the ring, but no [N II] λ6583 line was seen. Since [N II] quite generally accompanies Hα in the spectra of extragalactic objects, this is rather surprising," especially since both lines could be seen in the spectrum of the brighter component A.

The model predicts, further, that after complete separation from the central spheroid the spinning gas ring should be expanding under the effect of the unbalanced centrifugal force until enough additional gas has been swept up to slow down both rotation and expansion. Conservation of angular momentum during the expansion will also tend to reduce the rotational velocity. This is consistent with the average ring diameter in table 1, $\langle D \rangle$ = 12–24 kpc (for $h = 1$ or $\frac{1}{2}$), which is rather more than the mean diameter of 10–20 kpc of the H I annulus in the disks of spirals. A radius increase of 20 percent or 2–4 kpc in 5 $\times$ 10^7 years would imply an average expansion velocity of $\sim$40–80 km s^{-1}. This prediction could be checked by detailed spectroscopic observations of the velocity fields.

c) Morphological Characteristics

Depending on (i) the morphological type of the original galaxy (lenticular or spiral, ordinary or barred) and its stage (early or late) along the Hubble sequence, (ii) the density distribution in its H I disk, (iii) the angle of incidence and relative velocity V_0 of the disk with respect to the IGC, and (iv) the density and structure of the IGC, a great variety of appearances can be expected to result from the same basic encounter process. For example, the Mayall system (Arp 148) might suggest that the initial galaxy was a late-type barred spiral, since the barlike A component has an early (A7) spectral type (Smith 1941).

A ringed A component, as in IC 298 = Arp 147, suggests that the initial galaxy was an SA(r) type, perhaps similar to NGC 7702 (de Vaucouleurs and de Vaucouleurs 1961). Large narrow rings may arise from early-type spirals in which neutral hydrogen is apparently concentrated in a narrow outer annulus; a possible example is Arp 146. Broader rings may be produced by late-type spirals in which the central deficiency of hydrogen is minimal; Arp 148 (Mayall's object) is a possible example.

This model also accounts for the asymmetric intensity distribution which is a common characteristic of the rings. For example, in Arp 141, 146, 147, 148, and VII Zw 466 (fig. 2) one side of the ring is stronger than the other. This is easily understood since the initial velocity V_0 will not usually be simultaneously normal to the disk and to the cloud interface; one side of the disk will then collide with the IGC first, sweep up cloud matter, and be slowed down, while the opposite side will reach first contact some millions of years later. Since collisional excitation and star formation will start earlier on the leading side of the disk, it should be denser and appear brighter, as observed.

The angle of incidence between the initial galactic plane and the cloud interface will play a particularly important part in determining the subsequent appearance of the system. We note that, for Arp 146, 147, 148, I Zw 45, and VII Zw 466, the lenticular companion is often close to the *minor* axis of the ring. (This point has been made previously by Theys 1973.) This is consistent with rings resulting from nearby pole-on encounters of the galaxy with an IGC, as we would expect from the model. On the other hand, if V_0 is close to the plane of the original galactic disk, then the encounter could lead to peculiarly distorted shapes for the resulting object. Strong bending, crumpling, and "doubling up" of the original disk, aggravated by tidal distortion, could lead to objects of strange appearance—for example, Arp 142, 144, and 149 (see Appendix A).

d) Very Early and Late Phases

We ask whether examples of very early ($t < 10^7$ yr) and late ($t > 10^9$ yr) phases of the phenomenon could be recognized among peculiar galaxies, not otherwise explainable by conventional known effects such as tidal interaction or ejection.

We suggest that NGC 3646, a "strange spiral galaxy" (Burbidge, Burbidge, and Prendergast 1961), may represent an early stage of the separation between the central component and the outer spiral structure of an SA(rs)bc galaxy, originally similar to NGC 1068, 5055, or 6753. We note that (1) the nucleus of the small inner spiral pattern (component A) is displaced from the center of the disk isophotes, and in particular of of the unusually bright, broken ring in the outer spiral structure (component B); (2) the radial velocity of this nucleus (4185 km s^{-1}) differs by about 100 km s^{-1} from the mean velocity of symmetrically located points on the outer ring near the line of nodes (4065 and 4509 km s^{-1}, mean 4287; see fig. 2 of Burbidge *et al.* 1961). For $t < 10^7$ yr, the line-of-sight separation of the two components may be of the order of 1 kpc; if the transverse velocity difference is also of the order 100 km s^{-1}, then this could explain the displacement between the nucleus and the center of the outer ring.

Very late stages ($t > 10^9$ yr) will be more numerous but more difficult to identify, because they may closely resemble normal late-type or Magellanic systems. Indeed, it is possible that many late-type objects in the Sm–Im range were originally formed by the mechanism described here. These systems are characterized by (i) slower rotation, (ii) less flattening, (iii) smaller mass and average luminosity, (iv) greater ratio of hydrogen to total mass than galaxies of stage Sd and earlier (de Vaucouleurs 1973; Roberts 1969; Gouguenheim 1969). All these characteristics are consistent with the expected results of the collision between the spinning gas disk of a spiral galaxy and an IGC. This may also help to account for the presence of so many galaxies that "appear young in an evolutionary sense" (Sandage 1963) side by side with old systems.

Conversely, we suggest that at least some of the lenticular galaxies, which share with normal spirals (i) a high rate of spin, (ii) an extreme flattening, and (iii) a hydrogen-deficient spheroidal component, but lack the dense gaseous disk and young type I population of spirals, may be the stellar component remnants of spirals that have been swept clean of their gas disks by traversing IGCs.

We note that interaction between a visible galaxy and an optically invisible IGC may help explain some puzzling cases of apparent tidal distortion in seemingly isolated galaxies—for example, NGC 7135 (de Vaucouleurs and de Vaucouleurs 1961; de Vaucouleurs 1968) and Arp 179.

Finally, the IGC picture may be relevant to Searle and Sargent's (1970, 1972) "isolated extragalactic H II regions," of which I Zw 18 and II Zw 40 are two well-studied examples. These are dwarf optically compact galaxies, with masses of 10^8–10^9 $\mathfrak{M}_\odot$; there is no direct estimate of their H I size. They are somewhat underabundant in oxygen and neon relative to hydrogen, but have normal helium abundances. An unusually large fraction of their mass is apparently in the form of interstellar neutral hydrogen (Chamaraux, Heidmann, and Lauqué 1970). They infer that the present star formation rate in these galaxies greatly exceeds the average past rate, and that these systems are either young (in the sense that most of their star formation has occurred recently) or that star formation occurs in intense bursts separated by long quiescent periods. We will show in the next section that occasional encounters between two IGCs are likely. We can expect strong shocks to form at impact and propagate through the clouds (see, for example, Stone 1970). The resulting object may appear at a given time as a fairly compact isolated extragalactic H II region, embedded in an extended H I cloud; it would probably be underabundant in elements heavier than He, as observed in I Zw 18 and II Zw 40.

III. OBSERVATIONAL CONSTRAINTS

In this section, we discuss some observational constraints on the IGC picture, and estimate parameters (masses, radii, and number densities) of the typical cloud.

a) IGC Parameters

To estimate IGC parameters, we adopt the following values:

i) $H_0 = 100h$ km s^{-1} Mpc^{-1} ($h = H/100$), so that

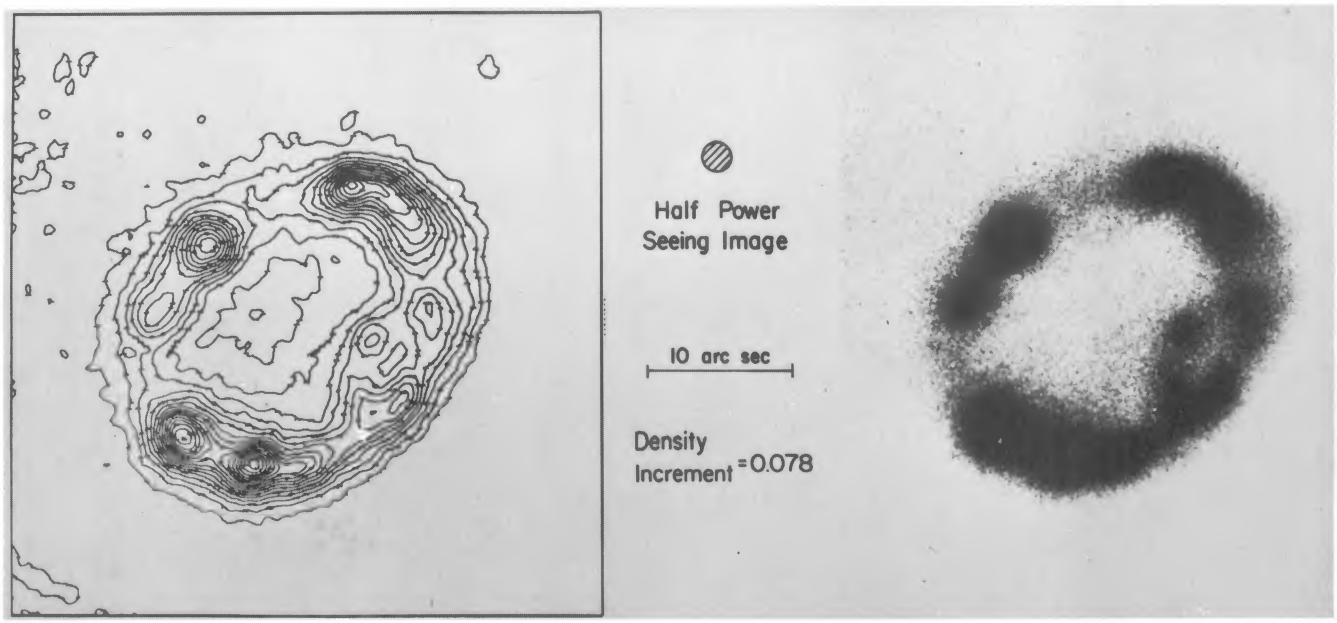

FIG. 2.—Isodensity contours of ring component B of VII Zw 466 from electronograph by G. Chincarini and H. M. Heckathorn. Note low-level luminosity inside ring and that minimum is not at geometric center of ring.

the critical cosmic mass density $\rho_0 = 3H_0^2/8\pi G = 2.78h^2 \times 10^{11}\,\mathfrak{M}_\odot\,\mathrm{Mpc}^{-3} = 1.88h^2 \times 10^{-29}\,\mathrm{g\,cm}^{-3} = 8h^2 \times 10^{-6}$ H atoms cm^{-3} for He/H = 0.1.

ii) Allowing for a plausible, but uncertain, incompleteness factor, we estimate from table 1 (see Appendix B) that there are about 30 ring-type galaxies with redshifts $\leq 1/30$, i.e., within a distance $\Delta = 100h^{-1}$ Mpc. Their space density is then $N_R \simeq 7 \times 10^{-6}h^3$ Mpc^{-3}.

iii) In our picture we would expect the visible ring-type systems to originate from spirals of types S0/a to Sd which comprise about half the total population in the top five magnitudes of the galaxy luminosity function (Appendix B); these include spirals with masses larger than about $10^{10}\,\mathfrak{M}_\odot$ (Roberts 1969; Heidmann 1969). From Kiang (1961) we take the space density of these galaxies to be about $5 \times 10^{-2}h^3$ Mpc^{-3}.

iv) We believe that ring-type systems are identifiable for about $0.5 \times 10^8 h^{-1}$ yr; this follows from the mean projected linear separations ($\langle S \rangle \simeq 8.4h^{-1}$ kpc) and corrected differential radial velocities ($\langle \Delta V \rangle \simeq 150$ km s^{-1}) of the two components in table 1. If we assume that the space distribution of IGCs is statistically uniform, then it follows from (ii) and (iii) that the probability of encounter between a given spiral and an IGC is about 1.5×10^{-4} in $0.5 \times 10^8 h^{-1}$ yr.

v) From table 1 the typical rms relative radial velocity (corrected for observational errors) is $\langle \Delta V^2 \rangle^{1/2} = 170$ km s^{-1}. These numbers are all fairly uncertain, but they should be adequate for order of magnitude estimates of the IGC parameters from the following five constraints.

Let N be the mean number density of clouds, R and M the cloud radius and mass, and ρ the typical mean density within a cloud. We assume again that the IGCs are uniformly distributed in space, recognizing that the tests described in this section may lead us to relax this condition later (see Appendix C).

1) In $0.5 \times 10^8 h^{-1}$ yr a galaxy travels $8 \times 10^{-3}h^{-1}$ Mpc with respect to nearby IGCs, so its collision probability is $8 \times 10^{-3}h^{-1}N\pi R^2 = 1.5 \times 10^{-4}$ from (iv) above. Then

$$NR^2 \simeq 5.6 \times 10^{-3}h\ \mathrm{Mpc}^{-1}. \qquad (1)$$

2) We can estimate the minimum value of ρ such that the interstellar medium will be removed from the galaxy in a pole-on encounter with an IGC. The condition is that $\rho V^2 > \sigma k_z$, where σ and k_z are typical values of the surface density of the interstellar medium and of the force per unit mass perpendicular to the galactic plane. We take $\sigma = 5 \times 10^{-4}$ g cm^{-2} (Kerr and Westerhout 1965, fig. 13) and $k_z = 5 \times 10^{-9}$ cm s^{-2} (Oort 1965), which are appropriate for the Milky Way at the Sun's radius, as typical values in the annular zone of neutral hydrogen (see § II*a*); then with $\langle V^2 \rangle^{1/2} = 170$ km s^{-1},

$$\rho > \rho_c \equiv 8.7 \times 10^{-27}\,\mathrm{g\,cm}^{-3} = 1.3 \times 10^{14}\,\mathfrak{M}_\odot\,\mathrm{Mpc}^{-3}. \qquad (2)$$

3) To produce the observed phenomena, the average cloud radius R must be no smaller than the radius r of the typical H I ring in the galaxy; from table 1, where $\langle D \rangle = 2r = 12h^{-1}$ kpc (see also Hodge 1969), we take

$$R \geq r \simeq 6h^{-1}\ \ (\mathrm{kpc}). \qquad (3)$$

4) Another condition on R comes from the requirement that the galaxy remains in the cloud long enough for its interstellar matter to be removed. We can estimate this time roughly by assuming that k_z is constant and $\rho = \alpha\rho_c$, where ρ_c is given by equation (2). Then the time for the interstellar layer to reach a height z above the galactic plane is

$$t = \left[\frac{2\sigma z}{(\alpha - 1)\rho_c V^2}\right]^{1/2} = \left[\frac{2z}{(\alpha - 1)k_z}\right]^{1/2}.$$

The condition $2R > Vt$ becomes $R > 3z^{1/2}(\alpha - 1)^{-1/2}$, where R and z are in kpc. Taking $z = 5$ kpc, say, the constraint is then

$$R > 7(\alpha - 1)^{-1/2}\ \ (\mathrm{kpc}). \qquad (4)$$

5) If we assume, finally, that the smoothed-out density of IGCs does not exceed the critical density ρ_0, then $NM < 2.8 \times 10^{11}h^2\,\mathfrak{M}_\odot\,\mathrm{Mpc}^{-3}$. Eliminating N between this inequality and equation (1) leads to

$$R\rho < 1.2 \times 10^{13}h\ \ (\mathfrak{M}_\odot\,\mathrm{Mpc}^{-2}). \qquad (5)$$

Figure 3 shows the constraints defined in the (R, ρ)-plane by the inequalities (2) to (5). Conditions (3) and (5) are calculated for the current limiting estimates $0.5 \leq h \leq 1.0$. The constraints confine the possible range of parameters to a small region around $R = 15$ kpc, $\rho = 2.5 \times 10^{14}\,\mathfrak{M}_\odot\,\mathrm{Mpc}^{-3} = 1.7 \times 10^{-26}$ g cm^{-3} $= 7 \times 10^{-3}$ atoms cm^{-3} (if the He/H number

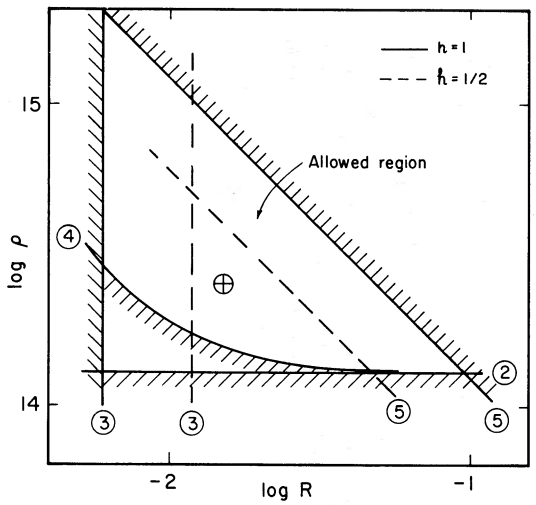

FIG. 3.—Constraints on parameters of intergalactic gas clouds in the (R, ρ)-plane defined by inequalities (2)–(5) for two values of $h = H_0/100$. Possible parameters are restricted to a small allowed region around ⊕, $R = 15$ kpc, $\rho = 2.5 \times 10^{14}\,\mathfrak{M}_\odot$ Mpc^{-3}, $\mathfrak{M} = 3 \times 10^9\,\mathfrak{M}_\odot$, and $N = 25h$ Mpc^{-3}.

ratio is 0.1), $\mathfrak{M} = 3 \times 10^9\,\mathfrak{M}_\odot$, and $N = 25h$ Mpc^{-3}.

We can now estimate the cloud-cloud encounter time. This time is $(N\pi R^2 \times 2 \times 10^{-10})^{-1}$ yr $= 3 \times 10^{11}h^{-1}$ yr. Although this is much longer than the Hubble time, we note that with $N = 25h$ Mpc^{-3} there will be about one encounter per Mpc^3 in $10^{10}h^{-2}$ yr. As we suggested in the previous section, these encounters could be relevant to the dwarf ($M > -16$) emission-line galaxies. Sargent (1972) estimates their space density as about 10^{-2} Mpc^{-3}. Our estimated encounter rate for IGCs would then be consistent with this space density if the burst of star formation following the encounter lasted about 10^8 yr, and this seems entirely reasonable.

Now we need to consider whether the IGC picture stands up to the tests which give limits to the diffuse H I density in the Universe. First we discuss very briefly the equilibrium of an IGC.

b) Equilibrium of an IGC

With $R = 15$ kpc and $\mathfrak{M} = 3 \times 10^9\,\mathfrak{M}_\odot$, internal motions of about 30 km s^{-1} are required to keep the IGC in equilibrium. For example, the estimated mass of the H I companion to NGC 300 (Shobbrook and Robinson 1967), is in the range $10^8 < \mathfrak{M}/\mathfrak{M}_\odot < 10^9$, and the observed mean profile halfwidth is 30 km s^{-1}. It is not clear whether this is due to rotation or to a less ordered velocity field.

c) Emission

Penzias and Wilson (1969) placed an upper limit of 0.08° K on the step in the sky brightness temperature around 21 cm, arising from diffuse emission by intergalactic H I. Is our IGC picture consistent with this limit? Penzias and Wilson's measures covered a range of ± 2800 km s^{-1} about 1420 MHz, which corresponds to distances less than about 50 Mpc. With $N = 25h$ Mpc^{-3} there is a 50 percent chance of finding an IGC in the 2° diameter beam of their antenna within a distance of $4.0h^{-1/3}$ Mpc. We can estimate the peak brightness temperature T_b of an IGC from

$$T_b = 5.45 \times 10^{-14} N_{\rm H}/[\sigma(2\pi)^{1/2}]$$

where $N_{\rm H}$ is the typical number of H atoms cm^{-2} in the line of sight, and σ is their velocity dispersion (in cm s^{-1}) (see McGee and Milton 1966). For $n = 7 \times 10^{-3}$ cm^{-3}, $R = 15$ kpc and $\sigma = 30$ km s^{-1}; $T_b = 2.28$° K. Now at $4.0h^{-1/3}$ Mpc an IGC subtends $0.^\circ 4h^{1/3}$, so the corresponding antenna temperature is approximately $2.28(0.4h^{1/3}/2)^2 = 0.09h^{2/3}$ ° K, and this is at or below the Penzias and Wilson limit, depending on the value of h. More distant clouds contribute yet smaller fluctuations to T_b.

d) H I Absorption

Penzias and Scott (1968) place an observational limit of 5×10^{-4} on the optical depth of intergalactic H I in the direction of Cyg A. Cygnus A has a redshift of 0.056 corresponding to a distance of about $170h^{-1}$ Mpc. With $NR^2 = 5.6 \times 10^{-3}h$ Mpc^{-1}, we would expect about 3 ± 2 clouds to be in the line of sight to Cyg A. These would produce fairly narrow absorption lines in the spectrum of Cyg A. The typical optical depth for an IGC is

$$\tau = \frac{T_b}{(T_e - T_R)} = \frac{2.28}{(T_e - T_R)},$$

where T_e is the excitation temperature and T_R is the radiative temperature of the cosmic microwave background. This is probably larger than the 5×10^{-4} limit. On the other hand, the line width is about 0.3 MHz, while the radiometer bandwidth was 1 MHz; also the total range surveyed was about 8000 km s^{-1}, which reduces the expectation to one or two clouds only. It seems unlikely that IGCs of the type postulated here would have been detected by the Penzias-Scott experiment.

e) Absorption Features in QSO Spectra

If high-redshift QSOs are at their cosmological distances, then IGCs should be seen in absorption in QSO spectra, at Lα and 21 cm. For $R = 15$ kpc and $n = 7 \times 10^{-3}$ cm^{-3}, the column density of H I atoms for a line passing through the center of an IGC is about 6×10^{20} cm^{-2}: the resulting Lα and 21-cm absorption features should be readily detectable. From Bahcall and Peebles (1969), the number of IGCs along the line of sight between z_1 and z_2 is (for $q_0 = \frac{1}{2}$)

$$p = [\tfrac{2}{3}\pi R^2 N c H_0^{-1}][(1 + z_2)^{3/2} - (1 + z_1)^{3/2}]. \quad (6)$$

First consider Lα: high-redshift absorption-line QSOs have many unidentified absorption lines shortward of Lα at the emission-line redshift. For example, Lynds (1971) tabulates 70 absorption lines in the spectrum of 4C 05.34 ($z = 2.88$) between λ3500 and Lα, at least 43 of which remain unidentified. From equation (6), we would expect about 100 IGCs in the redshift interval $z = 2.88$ to $z = 1.88$ (the redshift of Lα at λ3500). Lynds (1972) suggests that these unidentified lines may be due to Lα from clouds that do not produce other detectable features. Morton and Morton (1972) fitted Voigt profiles to unidentified lines shortwards of Lα in the spectrum of PHL 957 ($z = 2.69$), assuming these lines are in fact Lα. They infer velocity halfwidths of about 40 km s^{-1}, but column densities of only 10^{14} to 10^{15} cm^{-2}.

Brown and Roberts (1973) searched the spectrum of 3C 286 ($z = 0.85$) for 21-cm absorption features between $z = 0.86$ and $z = 0.68$, and found one at $z = 0.69$. It has a profile halfwidth of 8 km s^{-1} and a column density of 3×10^{20} cm^{-2} for an assumed spin temperature of 100° K. From equation (6), we would expect about 12 ± 4 IGCs along the line of sight in this redshift interval.

In summary, our IGC picture is consistent with the standard tests for intergalactic neutral hydrogen, except that it may be in trouble with data on absorption features in QSO spectra (if QSOs are at currently assumed distances). We recognize this, and anticipate

that future data will soon show whether the picture remains tenable or needs modification.

IV. CONCLUSION

1. We propose that the ring-type galaxies result from the interaction of normal spiral galaxies with intergalactic clouds. These clouds have typical masses of $3 \times 10^9\,\mathfrak{M}_\odot$, radii of 15 kpc, and space density $25h\ \mathrm{Mpc}^{-3}$.

2. Smart (1973) and Silk and Tarter (1973) have discussed the stabilizing of clusters of galaxies by intergalactic clouds. Silk and Tarter invoke ionized clouds, and find that the cloud parameters are restricted to a fairly narrow range by stability requirements and observations of background radiation: for small clusters or groups, their clouds have $10 < R < 100$ kpc and $10^9 < \mathfrak{M}/\mathfrak{M}_\odot < 10^{10}$. These parameters, derived from quite different considerations, are similar to those for the IGCs discussed here. It will be necessary to explain why the IGCs should have these particular parameters; as Silk and Tarter point out, the masses are similar to those of dwarf galaxies.

3. From § III(*a*) an individual spiral has a 3 percent chance of encountering an IGC in 10^{10} yr. Compare this with the 25 percent relative frequency of lenticular galaxies among disk galaxies in a sample of 1500 bright galaxies (de Vaucouleurs 1963, table 2). It seems possible that a significant fraction of lenticular systems has been produced in this way, especially if the space density of galaxies and IGCs was significantly higher in the past (since the collision rates are proportional to N^2).

4. Detailed photometric and spectroscopic observations of ring-type galaxies and their spheroidal companions and detailed evaluation of quantitative models are needed to test our hypothesis. The search for 21-cm emission from and absorption by IGCs is particularly important here; our assumptions that the IGCs are neutral and uniformly distributed may need to be modified in the light of such observations. For example, it may well be that IGCs are clustered around the visible galaxies. We will show in Appendix C that this does not change significantly the constraints calculated in § III but considerably eases the problem of the absorption features in QSO spectra.

Some of the ideas in this paper originate from discussions of one of the authors (K. F.) with Professor N. J. Woolf in 1966. We are very grateful to him for this impulse, although he is in no way responsible for any errors in our developments. Our appreciation goes to Dr. G. Chincarini for allowing us to use his photograph and contour map of VII Zw 466. The similarity of the latter to H I contour maps of spirals directed the second author's attention to the problem. We also thank Dr. H. C. Arp for permission to reproduce figures from his Atlas and Dr. A. W. Rodgers for valuable discussion and comments.

APPENDIX A

A POSSIBLE INTERPRETATION OF NGC 7828–29 = ARP 144

Consider the case of an ordinary spiral, SA(s)b, similar to M31, colliding with a *dense* IGC ($\rho \simeq 10^{-25}\ \mathrm{g\ cm}^{-2}$) so that the stopping length is small compared with the radius $R \simeq 10$ kpc of the H I annulus in its disk. Assume that the relative velocity vector $V \simeq 200\ \mathrm{km\ s}^{-1}$ forms small angles, say $< 30°$, with both the plane of the disk and the cloud interface (fig. 4). With this geometry the collision starting at point A on the leading edge of the disk will lift the H I annulus out of the disk and, so to speak, progressively "peel it back" above the disk as the stellar component of the galaxy penetrates more and more deeply into the IGC while the gas ring is stopped close to the impact interface. Three typical phases of the phenomenon are illustrated in figures 5*a*, 5*b*, and 5*c*. In (*a*), shortly after first contact, only a small part (*BAH*) of the galactic disk has penetrated the IGC (~ 2 kpc in $\sim 10^7$ yr) and a short arc (*BA'H*) of the H I ring has been lifted off the disk and remains close to the cloud interface; in (*b*), some $\sim 5 \times 10^7$ yr later, the nucleus of the galaxy has reached the cloud interface and half the H I ring (*CB'A'H'G*) has been removed from the disk; attraction from the stellar component of the galaxy (including ~ 95 percent or more of the initial mass) causes the raised part of the ring to curl back toward the galactic plane (arc *C'A'H'*); in (*c*) after some $\sim 8 \times 10^7$ years, three-quarters of the disk is immersed in the IGC, only one-quarter of the H I ring is still in the disk; the rest has been removed from it along an arc (*DC'B'A'H'G'F*) whose apex near *A'* is falling back toward the galactic plane near *A*, its motion being resisted and slowed down by the gas cloud in which it is still immersed. Phase (*c*) bears an obvious resemblance to the present aspect of NGC 7828–29 (fig. 6). It is also clear that after total immersion of the system in the IGC, component A will look very much like a normal S0 galaxy, similar to NGC 5102 (de Vaucouleurs 1956, fig. 18; Sérsic 1968, p. 39), except perhaps for its weaker disk. Lenticulars with unusually weak disks are known to exist; an example is NGC 5365 (de Vaucouleurs 1956, fig. 21).

The perspective in figures 4 and 5 was chosen to approximately match the aspect (inclination of disk and angle of *V* to line of sight) of NGC 7828. From other viewpoints and with slightly different impact parameters (ψ, θ, *V*) very different appearances may result from the same basic phenomenon; for example an observer in the *Oz* direction in the plane normal to the line of nodes *DF* of the disk and the IGC interface, looking at phase (*c*) might see something rather similar to NGC 2936–37 (Arp 142). Here the original galaxy was perhaps a ring-type barred spiral, SB(r),

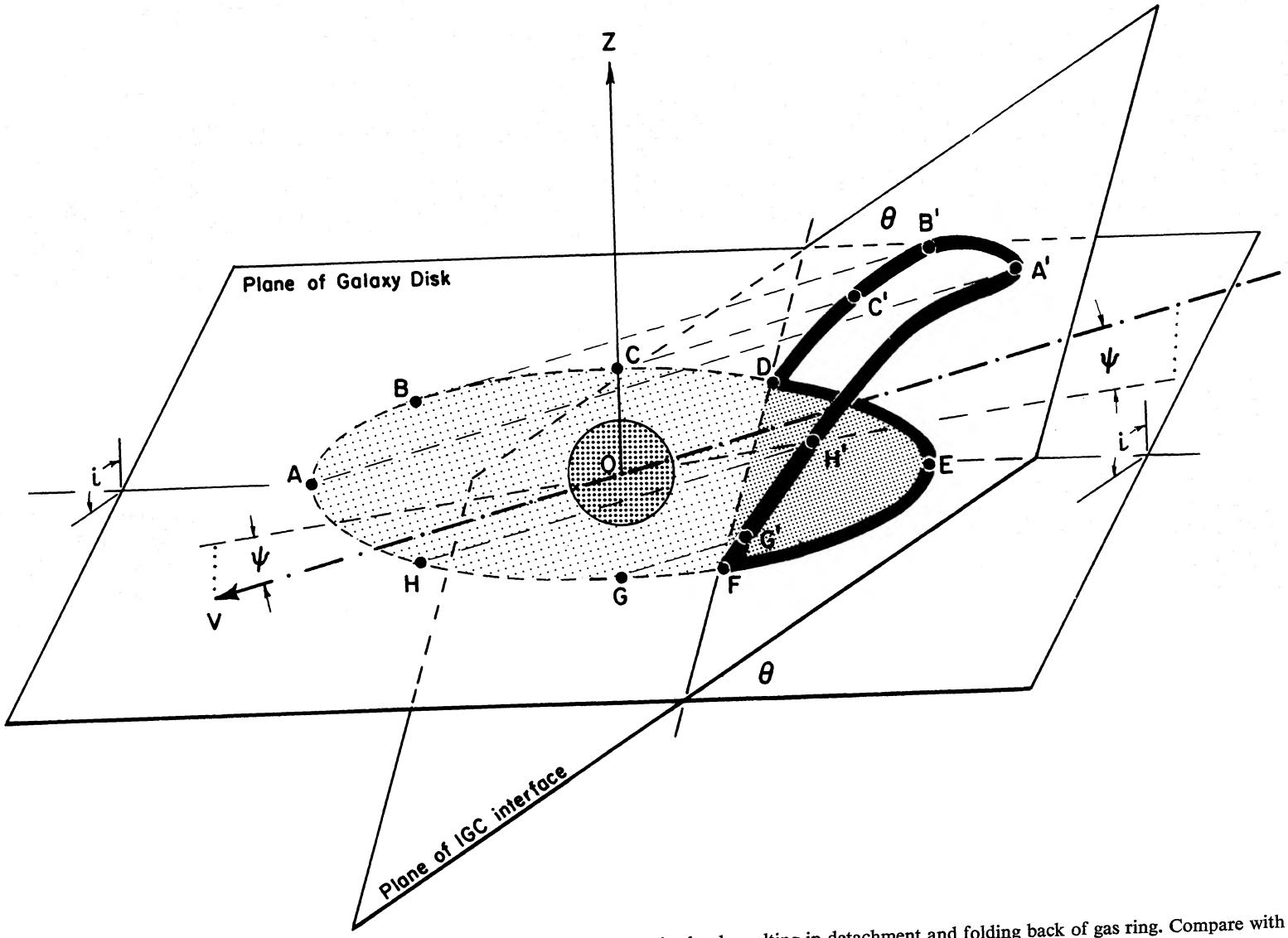

FIG. 4.—Geometry of collision between disk galaxy and interface of intergalactic cloud resulting in detachment and folding back of gas ring. Compare with figs. 5 and 6.

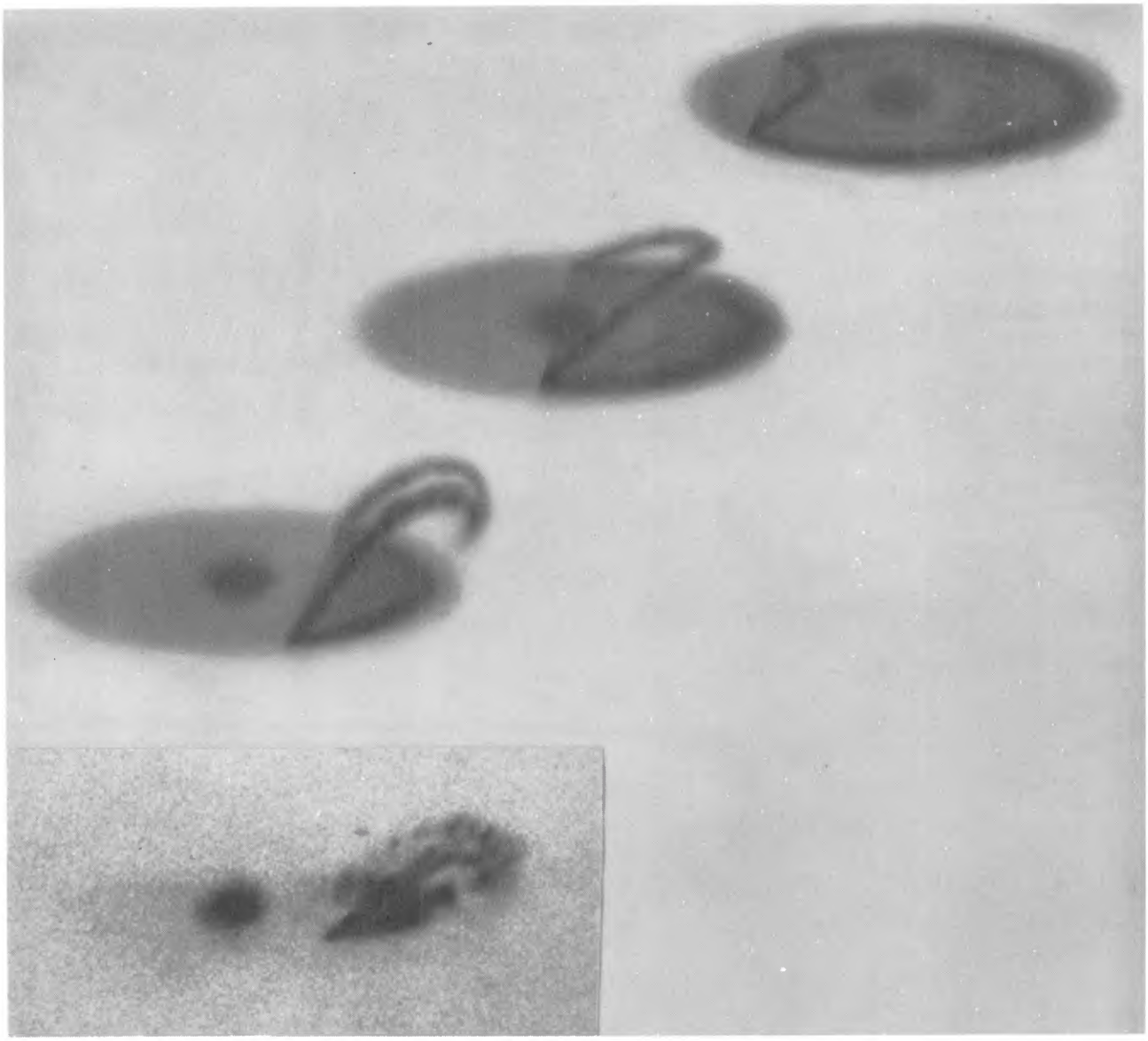

FIG. 5. (*top*)—Artist's conception of three typical phases of penetration of disk galaxy in IGC with progressive separation of gas annulus from disk. Artwork by J. Roth.

FIG. 6 (*bottom*).—Photograph of NGC 7828–29 = Arp 144 reproduced from Arp (1966). Hale Observatory photograph with 5-meter reflector.

similar to NGC 1433 or 1512 (de Vaucouleurs 1956). Differences in the initial morphological types of the galaxies, in the shapes of the IGCs and in the relative masses, dimensions, and velocities of the two colliding objects and their space orientations will cause a great variety of aspects. Tidal interactions between the galactic nucleus, the displaced ring, and the IGC will further complicate individual cases. Finally the dynamic and physical evolution of the gas ring remnant (component B) after complete separation add still more complications to the simple basic picture.

APPENDIX B

SPACE DENSITIES AND COLLISION PROBABILITIES

The IGC parameters depend critically on the collision probability p between spirals and IGCs, which in turn depends on the space densities of spirals and ring systems. The latter can be estimated as follows. Nine of the 15 objects in table 1 have a redshift $z \leq 1/30$ ($V_0 \leq 10^4$ km s^{-1}), i.e., are within a radius of $100h^{-1}$ Mpc and a volume $4.2 \times 10^6 h^{-3}$ Mpc^3; this gives a lower limit to the space density of ring systems, $N_R > 2 \times 10^{-6} h^3$ Mpc^{-3}. If all 15 systems are at $z \leq 1/30$ (which seems likely from their apparent diameters), then $N_R \geq 3.5 \times 10^{-6}$ Mpc^{-3}. Allowing for a conservative incompleteness factor of 2 (i.e., 30 ring systems with $z \leq 1/30$), we estimate $N_R = 7 \times 10^{-6} h^3$ Mpc^{-3}.

The space density of giant galaxies in the top five magnitudes of the luminosity function ($0 < x < 5$) is $N_G = 1 \times 10^{-1} h^3$ Mpc^{-3}, after Kiang (1961), and about half of these galaxies are spirals in the S0/a to Sc/d range of the Hubble sequence (de Vaucouleurs 1963), so the space density of spirals $N_S = 5 \times 10^{-2} h^3$ Mpc^{-3}. It follows that the probability of an encounter between a given spiral and an IGC is

$$p = N_R/N_G = 1.5 \times 10^{-4}$$

in $0.5 \times 10^8 h^{-1}$ yr, the time interval during which ring systems remain recognizable, as estimated from $\langle S \rangle$ and $\langle \Delta V \rangle$ in table 1. This corresponds to a collision frequency of $3 \times 10^{-12} h$ yr^{-1}.

APPENDIX C

ESTIMATE OF IGC PARAMETERS, IF THE CLOUDS ARE CLUSTERED AROUND SPIRALS

In § III*a*, we estimated IGC parameters, assuming that the IGCs are uniformly distributed in space. Now we re-estimate these parameters, assuming that the IGCs tend to be clustered around spirals, perhaps like dwarf galaxies (Reaves 1956; van den Bergh 1959, 1966; de Vaucouleurs 1965).

Conditions (1)–(4) are unchanged. Condition (1) is more elegantly derived as $N\pi R^2 \langle S \rangle = 1.5 \times 10^{-4}$, independent of V, so $NR^2 = 5.6 \times 10^{-3} h$ Mpc^{-1}. To derive a condition corresponding to (5), we need some limits for the mass of IGCs per galaxy.

1. An upper limit to the aggregate mass density of IGCs per spiral is obtained by assuming that they account for the missing mass in groups dominated by spirals, which is 1.5 orders of magnitude greater than the rotational mass of the visible galaxies (de Vaucouleurs 1960, 1974). This is probably an extreme upper limit since intergalactic hydrogen has not been detected in groups (Gott, Wrixon, and Wannier 1973) and not all groups are stable (de Vaucouleurs 1959; Turner and Sargent 1974). (We should note, however, that the three groups 6, 12, 51 observed by Gott *et al.* all have crossing times of the order of the Hubble time; this suggests that they are not gravitationally bound as discussed by Turner and Sargent.)

We will consider in turn two possible assumptions: (*a*) the system of clouds around each galaxy is in stable dynamical equilibrium, (*b*) it is not.

From the groups discussed by Rood, Rothman, and Turnrose (1970), we take the 17 groups with crossing time $\tau_c \lesssim 7 \times 10^9$ yr; these are the most likely to be dynamically bound. The typical group in this sample has 5 giant galaxies ($M_B < -18$), virial mass $\mathfrak{M}_V \simeq 10^{13} h^{-1} \mathfrak{M}_\odot$, characteristic radius $R \simeq 0.6 h^{-1}$ Mpc, and luminous mass $\mathfrak{M}_L \simeq 4 \times 10^{11} h^{-2} \mathfrak{M}_\odot$. This corresponds to $2 \times 10^{12} h^{-1} \mathfrak{M}_\odot$ of hidden matter per galaxy. We take this as an upper limit on the mass of IGCs per galaxy.

a) Now consider an individual galaxy immersed in a spherical cloud system of IGCs: $\mathfrak{M} < 2 \times 10^{12} h^{-1} \mathfrak{M}_\odot$ is the mass of this system, $\mathfrak{R}$ its radius, and V its velocity dispersion. Take $V = 170$ km s^{-1} again, and assume the cloud is in statistical *dynamical equilibrium.* (IGCs dominate the mass of the system.) Then $\mathfrak{R} \simeq G\mathfrak{M}/V^2$. Now let N (Mpc^{-3}) be the space density of IGCs around the galaxy, ρ ($\mathfrak{M}_\odot$ Mpc^{-3}) and R (Mpc) the density and radius of an individual IGC, as before. Then

$$\tfrac{4}{3}\pi N \mathfrak{R}^3 \times \tfrac{4}{3}\pi R^3 \rho = \mathfrak{M}$$

and $\rho R = 8 \times 10^{14} h^{-1} (2 \times 10^{12}/\mathfrak{M})^2$ ($\mathfrak{M}_\odot$ Mpc^{-2}). This constrains us to very large IGC masses: $M = 4\pi\rho R^3/3 = 3 \times 10^{15} h^{-1} (2 \times 10^{12}/\mathfrak{M})^2 R^2 \mathfrak{M}_\odot$. For the minimum values of R from equation (3), $M > 10^{11} h^{-1} \mathfrak{M}_\odot$. Such clouds would be difficult to stabilize in any plausible way.

b) Now *relax the requirement of equilibrium* for the system of IGCs: say the time for an IGC to cross the system is $\tau_c > 10^{10}$ yr, so $\mathfrak{R}$, $\mathfrak{M}$, and V are not related by the virial theorem. Now $\tau_c \simeq (G\langle\rho\rangle)^{-1/2}$, where $\langle\rho\rangle$ is the smoothed-out density of the system, so $\tau_c > 10^{10}$ yr means that $\langle\rho\rangle < 2 \times 10^{12}\,\mathfrak{M}_\odot\,\mathrm{Mpc}^{-3}$. The radius of the system of mass $\mathfrak{M}$ is then $\mathfrak{R} > 0.6(\mathfrak{M}/2 \times 10^{12})^{1/3}$ Mpc. A larger limit on $\mathfrak{R}$ comes from $\mathfrak{R} = V\tau_c > 1.7$ Mpc.

Then $V = 170\ \mathrm{km\ s^{-1}}$, $\mathfrak{R} > 1.7$ Mpc, $\mathfrak{M} < 2 \times 10^{12}h^{-1}\,\mathfrak{M}_\odot$ are consistent with $\tau_c > 10^{10}$ yr. Again, we have

$$\mathfrak{M} = N\tfrac{4}{3}\pi\mathfrak{R}^3 \cdot \tfrac{4}{3}\pi R^3\rho\,; \qquad \text{(C1)}$$

so with equation (1),

$$R\rho < 4 \times 10^{12}h^{-2}\,\mathfrak{M}_\odot\,\mathrm{Mpc}^{-2}\,. \qquad \text{(C2)}$$

From the constraints in figure 3, we see that the model breaks down if $\rho R \lesssim 3 \times 10^{12}h^{-1}\,\mathfrak{M}_\odot\,\mathrm{Mpc}^{-2}$, i.e., $\mathfrak{R}$ cannot be much larger than 1.7 Mpc nor, from equation (A1), $\mathfrak{M}$ much smaller than $2.10^{12}h^{-1}\,\mathfrak{M}_\odot$. It is perhaps noteworthy that this limit on $\mathfrak{R}$ turns out to be about twice the observed average limiting radius of nearby groups of galaxies (de Vaucouleurs 1965). The numerical constraints given by condition (8) for $\frac{1}{2} \leq h \leq 1$ are not significantly different from our original condition (5), and we adopt the same IGC parameters.

We now calculate the number of IGCs cut by a line of sight between z_1 and z_2 as in § III*e*. We adopt $\mathfrak{R} = 1.7$ Mpc, $R = 15$ kpc, $N = 25h\,\mathrm{Mpc}^{-3}$, $M = 3 \times 10^9\,\mathfrak{M}_\odot$, $\mathfrak{M} = 2 \times 10^{12}h^{-1}\,\mathfrak{M}_\odot$ as a set of parameters consistent with the constraints. We now have systems of IGCs, each system around an individual spiral. Let P_1 be the number of systems cut by the line of sight, and P_2 be the number of IGCs cut by a line through a system. From equation (6), and noting that the mean path length through a sphere of radius $\mathfrak{R}$ is $4\mathfrak{R}/3$, we have

$$P_1 \simeq \tfrac{2}{3}\pi(1.7)^2 \times 5 \times 10^{-2}h^3(3000/h)[B] \simeq 900h^2[B]\,,$$

where $[B] = [(1 + z_2)^{3/2} - (1 + z_1)^{3/2}]$,

$$P_2 \simeq \tfrac{4}{3}\mathfrak{R} \cdot N\pi R^2 = 0.04h\,,$$

so that

$$P_1P_2 = 36h^3[B]\,.$$

In the uniformly distributed case, we had $P = 35[B]$, from equation (6). Then $P_1P_2 \simeq Ph^3$; hence, if $h = \frac{1}{2}$, $P_1P_2 \simeq \frac{1}{8}P$ and the number of absorption features in QSO spectra no longer raises serious difficulties.

2. Another approach that we used in § III*a* is to assign enough mass to the IGCs associated with each galaxy to close the Universe (although we realize that injecting a cosmological assumption into the discussion is at best risky).

With $N_S = 5 \times 10^{-2}h^3\,\mathrm{Mpc}^{-3}$, the mass $\mathfrak{M}$ per galaxy needed to close the Universe is $5 \times 10^{-2}h^3\,\mathfrak{M} = 2.8 \times 10^{11}h^2\,\mathfrak{M}_\odot$ or $\mathfrak{M} = 5 \times 10^{12}h^{-1}\,\mathfrak{M}_\odot$. This is not sufficiently different from the value of $\mathfrak{M}$ in § 1 above to make us expect different conclusions.

REFERENCES

Arp, H. C. 1966, *Atlas of Peculiar Galaxies* (Pasadena: California Institute of Technology), and *Ap. J. Suppl.*, **14**, 1.
———. 1967, *Ap. J.*, **148**, 321.
Bahcall, J. N., and Peebles, P. J. E. 1969, *Ap. J.* (*Letters*), **156**, L7.
Baldwin, J. 1974, *M.N.R.A.S.*, in press.
Brown, R. L., and Roberts, M. S. 1973, *Ap. J.* (*Letters*), **184**, L7.
Burbidge, E. M. 1964, *Ap. J.*, **140**, 1617.
———. 1972, *ibid.*, **171**, 253.
Burbidge, E. M., and Burbidge, G. R. 1959, *Ap. J.*, **130**, 12 and 23.
Burbidge, E. M., Burbidge, G. R., and Prendergast, K. H. 1961, *Ap. J.*, **134**, 237.
Cannon, R. D., Lloyd, D., and Penston, M. V. 1970, *Observatory*, **90**, 153.
Chamaraux, P., Heidmann, J., and Lauqué, R. 1970, *Astr. and Ap.*, **8**, 424.
Chincarini, G., and Rood, H. J. 1972, *A.J.*, **77**, 4.
Davies, R. D. 1973, *IAU Symposium 58*, in press.
de Vaucouleurs, G. 1956, *Mem. Com. Obs. Mt. Stromlo*, Vol. **3**, No. 13.
———. 1959, *Ap. J.*, **130**, 718.
———. 1960, *ibid.*, **131**, 585.
———. 1963, *Ap. J. Suppl.*, No. 74.
———. 1968, *IAU Symposium No. 29: Nonstable Phenomena in Galaxies*, in Russian, Byurakan, 1966 May 4–12 (Yerevan: Armenian Academy of Science).
———. 1973, *IAU Symposium 58*, in press.
———. 1965, preprint of chapter to be published in "Stars and Stellar Systems," Vol. 9, ed. A. and M. Sandage and J. Kristian (Chicago: University of Chicago Press) (in press).
de Vaucouleurs, G., and de Vaucouleurs, A. 1961, *Mem. R.A.S.*, **68**, 69.
Field, G. B. 1972, *Ann. Rev. Astr. and Ap.*, **10**, 227.
Freemah, K. C., and Craft, J. L. 1974, to be published.
Gott, G. R., Wrixon, G. T., and Wannier, P. 1973, *Ap. J.*, **186**, 777.
Gottesman, S., and Davies, R. D. 1970, *M.N.R.A.S.*, **149**, 263.
Gouguenheim, L. 1969, *Astr. and Ap.*, **3**, 281.
Gunn, J. E., and Peterson, B. A. 1965, *Ap. J.*, **142**, 1633.
Heidmann, N. 1969, *Ap. Letters*, **3**, 153.
Hodge, P. 1969, *Ap. J.*, **155**, 417.
Humason, M. L., Mayall, N. U., and Sandage, A. R. 1956, *A.J.*, **61**, 97.
Kerr, F. J., and Westerhout, G. 1965, in *Stars and Stellar Systems*, Vol. 5, ed. A. Blaauw and M. Schmidt (Chicago: University of Chicago Press), p. 167.
Kiang, T. 1961, *M.N.R.A.S.*, **122**, 263.
Lynds, C. R. 1971, *Ap. J.* (*Letters*), **164**, L73.
———. 1972, *IAU Symposium 44, External Galaxies and Quasi-Stellar Objects*, ed. D. S. Evans (Reidel: Dordrecht), p. 127.
Mathewson, D. S., Cleary, M., and Murray, J. 1973, *IAU Symposium 58*, in press.
McGee, R. X., and Milton, J. A. 1966, *Australian J. Phys.*, **19**, 343.
Menzel, D., Whipple, F., and de Vaucouleurs, G. 1973, *Survey of the Universe* (Englewood Cliffs, N.J.: Prentice Hall), p. 788.
Morton, D. C., and Morton, W. A. 1972, *Ap. J.*, **174**, 237.
Oort, J. 1965, in *Galactic Structure*, ed. A. Blaauw and M. Smith (Chicago: University of Chicago Press), chap. 21.
Penzias, A. A., and Scott, L. H. 1968, *Ap. J.* (*Letters*), **153**, L7.
Penzias, A. A., and Wilson, R. A. 1969, *Ap. J.*, **156**, 799.
Reaves, G. 1956, *A.J.*, **61**, 69.
Roberts, M. S. 1969, *A.J.*, **74**, 859.
Rood, H. J., Rothman, V. C. A., and Turnrose, B. E. 1970, *Ap. J.*, **162**, 411.
Sandage, A. 1963, *Ap. J.*, **138**, 863.
Sargent, W. L. W. 1970, *Ap. J.*, **160**, 405.

Sargent, W. L. W. 1972, *Ap. J.*, **173**, 7.
Searle, L., and Sargent, W. L. W., 1970, *Ap. J.* (*Letters*), **162**, L155.
———. 1972, *Ap. J.*, **173**, 25.
Sérsic, J. L. 1968, *Atlas de Galaxias Australes* (Cordoba: Observatorio Astronómico).
———. 1970, in *Periodic Orbits, Stability, and Resonances*, ed. G. E. O. Giacaglia (Reidel: Dordrecht), p. 314.
Shobbrook, R. R., and Robinson, B. J. 1967, *Australian J. Phys.*, **20**, 131.
Silk, J., and Tarter, J. 1973, *Ap. J.*, **183**, 387.
Smart, N. C. 1973, *Astr. and Ap.*, **24**, 171.
Smith, R. T. 1941, *Pub. A.S.P.*, **53**, 188.
Stone, M. E. 1970, *Ap. J.*, **159**, 277, 293.
Theys, J. 1973, unpublished thesis, Columbia University.
Turner, E. L., and Sargent, W. L. W. 1974, *Ap. J.*, in press.
van den Bergh, S. 1959, *Pub. D. Dunlap Obs.*, Vol. **2**, No. 5.

G. DE VAUCOULEURS: Department of Astronomy, The University of Texas, Austin, TX 78712

K. C. FREEMAN: Mount Stromlo and Siding Spring Observatory, Woden, P.O., ACT 2606, Australia